Relationships of CO_2 assimilation rates with exposure- and flux-based O_3 metrics in three urban tree species

Yansen Xu [a,b], Bo Shang [a,b], Xiangyang Yuan [a,b], Zhaozhong Feng [a,b,*], Vicent Calatayud [a,c]

[a] State Key Laboratory of Urban and Regional Ecology, Research Center for Eco-Environmental Sciences, Chinese Academy of Sciences, Shuangqing Road 18, Haidian District, Beijing 100085, China
[b] College of Resources and Environment, University of Chinese Academy of Sciences, Beijing 100049, China
[c] Fundación CEAM, c/ Charles R. Darwin 14, Parque Tecnológico, 46980 Paterna, Valencia, Spain

HIGHLIGHTS

- Three greening species were exposed to 5 O_3 concentrations in 15 open-top chambers.
- A stomatal multiplicative model was individually parameterized for the three species.
- Concentration and flux-based O_3 response relationships for A_{sat} were established.
- The performance of both types of metrics for risk assessment was similar for any species.
- Current ambient O_3 concentration in China damages plant photosynthesis.

GRAPHICAL ABSTRACT
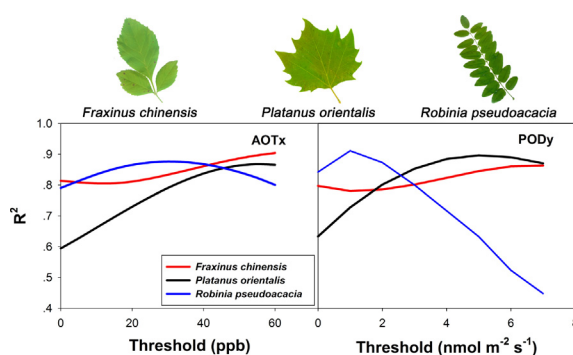
Fraxinus chinensis   *Platanus orientalis*   *Robinia pseudoacacia*

ABSTRACT

The relationships of CO_2 assimilation under saturated-light conditions (A_{sat}) with exposure- (AOTX, Accumulated Ozone exposure over a hourly Threshold of X ppb) and flux-based (POD_Y, Phytotoxic Ozone Dose over a hourly threshold Y $nmol \cdot m^{-2} \cdot s^{-1}$) O_3 metrics was studied on three common urban trees, *Fraxinus chinensis* (FC), *Platanus orientalis* (PO) and *Robinia pseudoacacia* (RP). Parameterizations for a stomatal multiplicative model were proposed for the three species. RP was the species showing lower species-specific maximum stomatal conductance (g_{max}) and experiencing lower cumulative O_3 uptake along the experiment, but in contrast it was the most sensitive to O_3. POD_Y was slightly better than AOTX metric at estimating relative A_{sat} (R-A_{sat}) for PO and RB but not for FC. The best fittings obtained for the regressions between R-A_{sat} and AOTX for FC, PO and RP were 0.904, 0.868, and 0.876, when the thresholds of X were 60 ppb, 55 ppb and 30 ppb, respectively. However, AOT40 performed also well for all of them, with R^2 always > 0.83. For POD_Y, the highest R^2 values for FC, PO and RB were 0.863, 0.897 and 0.911 at thresholds Y = 7, 5 and 1 nmol O_3 m^{-2} s^{-1}, respectively. Given the potentially higher O_3 removal capacity of FC and PO by stomatal uptake and their lower sensitivity to this pollutant than RP, the former two species would be appropriate for urban gardens and areas where O_3 levels are high. Parameterization and modeling of stomatal conductance for the main urban tree species may provide reliable estimations of the stomatal uptake of O_3 and other gaseous pollutants by vegetation, which may support decision making on the most suitable species for green urban planning in polluted areas.

© 2017 Elsevier B.V. All rights reserved.

* Corresponding author at: State Key Laboratory of Urban and Regional Ecology, Research Center for Eco-Environmental Sciences, Chinese Academy of Sciences, Shuangqing Road 18, Haidian District, Beijing 100085, China.
E-mail address: fzz@rcees.ac.cn (Z. Feng).

1. Introduction

Tropospheric ozone (O_3) is a secondary air pollutant of great concern for both human health and vegetation (The Royal Society, 2008).

Background O_3 levels have increased in the northern Hemisphere from 10 to 15 ppb to approximately 50 ppb (8-h summer seasonal average) since the end of the 19th century (The Royal Society, 2008). While the increase in yearly O_3 averages and has been recently stopped in some parts of the world as in Europe (Cooper et al., 2014), in Asia they are still increasing mainly due to rising NO_2 emissions associated with a fast economic growth (Cooper et al., 2014; Feng et al., 2015). In Europe and North-America, the recent reductions of NOx emissions in the cities have led to a parallel increase of the O_3 concentrations in urban areas (Sicard et al., 2013; Paoletti et al., 2014). It is well known that O_3 levels can be depleted locally in traffic areas due to a direct reaction with emitted NO, i.e. so called 'NOx titration effect' (The Royal Society, 2008). In cities, as it is the case of Beijing, the influence of traffic on urban O_3 levels can be best observed during weekends, when an increase of O_3 concentrations can be associated with a reduction in the circulating cars (Wang et al., 2015). Also, the areas far from traffic such as large gardens with abundant vegetation experience the highest hourly O_3 concentration, up to 50–65 ppb (Chen et al., 2015a). In some years the maximum monthly mean daily eight-hour average (MDA8) in Beijing area peaks above 75 ppb (Wang et al., 2017), with the summer period being the most polluted by O_3 (Chen et al., 2015b).

Urban trees play an important role in cities by reducing energy consumption of buildings by buffering the heat island effect, and by improving water and air quality among other ecosystem services and social benefits (Nowak, 2006; Nowak et al., 2014). As an example, in the central part of Beijing, the removal of pollutants by trees was quantified to be 1261.4 tons in 2002, mostly particles (61%), while O_3 accounted for 20% of the pollutants removed (Yang et al., 2005). As an important part of the gaseous pollutants including O_3 are taken up by the plants through the stomata (Cieslik et al., 2013), plants with higher stomatal conductance might be preferable for improving air quality in the cities. At the same time, tolerant species to the different pollutants should be selected (Gao et al., 2016). Finally, Biogenic Volatile Organic Compounds (BVOCs) emitted from vegetation such as isoprene and monoterpenes are precursors of O_3 and aerosols (The Royal Society, 2008; Loreto and Fares, 2013). Therefore, high BVOC emitter plants should be avoided in urban greening as their contribution to air urban pollution may even offset their removal capacity (Yang et al., 2005). The present paper provides information relevant to better understand the former two aspects in three common urban species in Chinese cities.

While many studies comparing the performance of exposure and O_3 flux metrics have considered tree biomass or growth as the key response variable for risk assessment (e.g., for establishing CLs), few have focused so far on establishing similar comparisons of both types of metrics based on responses of physiological variables such as photosynthetic parameters, pigment content or others (Bagard et al., 2015; Shang et al., 2017; Sun et al., 2014). While the interest on the effects of O_3 on tree growth or biomass is obvious given its economic relevance, the study of the responses of physiological variables may be complementary, as changes in some of these variables may be used as relevant indicators of early responses to O_3 (Bagard et al., 2015), with the advantage of being easy to measure by non-destructive methods. For the present study, we have selected the CO_2 assimilation rate under light-saturated conditions (A_{sat}) as the physiological response indicator, given that O_3 effects on CO_2 assimilation are very well known and largely documented (Wittig et al., 2007). The responses of A_{sat} against a range of O_3 exposures or accumulated fluxes are expected to provide relevant information on the sensitivity of the different species to this pollutant. The exposure metric used was the AOTX (accumulation over an hourly threshold O_3 concentration of X ppb), defined as the sum of the difference between the hourly mean O_3 concentration at the top of the canopy and X ppb for all daylight hours (when global radiation is >50 W m^{-2}) within a specified time period (LRTAP, 2017). The flux metric used was the POD_Y (Phytotoxic O_3 Dose over threshold Y nmol m^{-2} s^{-2}), calculated according to LRTAP (2017) methods. Among them, AOT40 and POD_1 are the most commonly used to establish the critical levels (CL) for protection of different receptor tree species (LRTAP, 2017). At the same time, we also investigated how these responses vary for different thresholds in both types of O_3 metrics, as thresholds have been related to the instantaneous O_3 flux detoxification capacity of the plants (Mills et al., 2011).

The main objectives of the present paper are: 1) to parameterize three common urban species for a stomatal conductance model; 2) to calculate exposure- and O_3 flux response relationships with A_{sat}, indicative of plant sensitivity to O_3; 3) to calculate which thresholds in both exposure and flux metrics are the most appropriate for establishing such responses, as well as the minimum O_3 concentrations contributing to such fluxes.

2. Material and methods

2.1. Experimental site and plant materials

The experiment was conducted in Yanqing (40°30′N, 116°E), north-west of Beijing in continental monsoon climate. One year old saplings of the Chinese ash (*Fraxinus chinensis* Roxb., FC), the oriental plane (*Platanus orientalis* L., PO) and the black locust (*Robinia pseudoacacia* L., RP) from a Hebei nursery were cultivated into 20 L circular plastic pots. Pots were filled with the soil that was taken from farmland at 0–10 cm depth, sieved out by a 0.3 mm pore mesh and then carefully mixed for homogeneity. Plants were pre-adapted to open-top chamber conditions for 10 days before O_3 fumigation.

2.2. Ozone treatments

The experiment was conducted in 15 open-top chambers (OTCs, octagonal base, 12.5 m^2 of growth space and 3.0 m of height, covered with toughened glass) with five treatments: charcoal-filtered ambient air (CF), non-filtered ambient air (NF), and NF with targeted O_3 addition of 20 (NF20), 40 (NF40), and 60 (NF60) ppb to develop the O_3 response relationships. Ozone concentrations within the OTCs were continuously monitored using an ultraviolet (UV) absorption O_3 analyzer (Model 49i; Thermo Scientific, Franklin, MA, USA), via a Teflon solenoid valve switch system, which collected air from sampling points at approximately 10 cm above the plant canopy during the experiment. The monitors were calibrated by a 49i–PS calibrator (Thermo Scientific) before the experiment and once a month during the experiment. Each treatment had three OTC replicates, and six potted plants of each species were exposed at each OTC. Fumigation lasted 96 days from 26 June to 30 September 2016. The daily maximum fumigation period was 10 h (from 08:00 to 18:00) when there was no rain, fog, mist, or dew. During the experiment all plants were watered at field capacity at 1–2 day intervals to avoid water stress.

During the experimental period (June 26 to September 30), the average O_3 concentrations (between 9:00 and 18:00) were 24.9 ppb, 45.5 ppb, 60.4 ppb, 75.7 ppb and 90.9 ppb for CF, NF, NF20, NF40 and NF60, respectively. The mean daily ambient temperature (T), relative air humidity (RH), photosynthetic photon flux density (PPFD) outside the OTCs were 24.9 °C and 69.7%, 841 µmol m^{-2} s^{-1}, collected by a CR1000 data logger (Campbell Scientific, North Logan, Utah, USA).

2.3. Gas exchange parameters

For the experiment, two datasets of gas exchange parameters were used. Stomatal conductance (g_s) was measured with a portable photosynthetic system (LI-6400XT, LICOR Corp, USA) in CF, NF and NF40 treatments, 3 times (8:00–10:00, 11:00–13:00 and 17:00–19:00) per day, on 7 different days between 06 July and 10 September 2016 under ambient light, temperature, humidity and CO_2 concentration conditions. This dataset composed of 648, 638 and 561, measurements for species FC, PO and RP, respectively, was used for parameterizing the different functions in the multiplicative model (Section 2.4), while hourly

averages were used to compare measured and modeled g_s values. On the other hand, A_{sat} was measured in two periods, in August and in September. We randomly selected three plants per species in each OTC, and one middle-level leaf from each plant (n = 30 for each species, i.e., 5 O_3 treatments × 3 OTCs × 2 measuring periods). During the measurements, photosynthetic active radiation (PAR) was set at 1200 µmol m^{-2} s^{-1}, CO_2 levels at 400 ppm, block temperature at 30–32 °C, and relative humidity (RH) between 45% and 55%. Measurements were carried out between 9:00 and 11:00 h on sunny days. This second dataset was used for estimating A_{sat}-AOTX and A_{sat}–POD$_Y$ relationships.

2.4. Ozone exposure and O_3 flux indices

The AOTX was calculated for thresholds 0 to 60 with steps of 5 ppb. The accumulated O_3 fluxes (POD$_Y$ over threshold Y nmol m^{-2} s^{-1}) were calculated following the Long-Range Transboundary Air Pollution methodologies for risk assessments as described in LRTAP (2017). For O_3 flux calculations, the leaf-level stomatal conductances for O_3 (g_{sto}) were first modeled and the resulting values were multiplied by the corresponding O_3 concentrations and a resistance term (Eq. (1)). Cumulative fluxes were finally calculated for the duration of the experiment (Eq. (3)).

The stomatal flux of O_3 (F_{st}, in nmol m^{-2} Projected Leaf Area (PLA) s^{-1}) was estimated for the upper surface of the laminar layer of the sunlit upper canopy leaves as follows:

$$F_{st} = [O_3] \cdot g_{sto} \cdot \frac{r_c}{r_b + r_c} \tag{1}$$

where $[O_3]$ is the O_3 concentrations at the top of the canopy (ppb), r_b is the quasi-laminar resistance (s m^{-1}) and r_c is the leaf surface resistance to O_3 (s m^{-1}), while g_{sto} is the stomatal conductance to O_3. For experimental conditions inside OTC the term $r_c / (r_b + r_c)$ can be considered negligible (Hu et al., 2015), and F_{st} can be calculated as the product of $[O_3]$ by g_{sto}.

To calculate g_{sto}, the Jarvis multiplicative model (Jarvis, 1976; Emberson et al., 2000) was applied, where g_{sto} is estimated from the functions that describe the response of stomata to key species-specific and environmental variables. Eq. (2) shows the g_{sto} model used in this study:

$$g_{sto} = g_{max} \cdot f_{phen} \cdot f_{light} \cdot \max[f_{min}, (f_{temp} \cdot f_{VPD})] \tag{2}$$

where g_{max} is the species-specific maximum stomatal conductance (mmol O_3 PLA s^{-1}) expressed on a Projected Leaf Area. Functions f_{phen}, f_{light}, f_{temp}, and f_{VPD}, all expressed in relative terms (i.e., values between 0 and 1), account for variation in g_{max} with leaf age, irradiance (µmol photons m^{-2} s^{-1}), air temperature (T, °C), and vapor pressure deficit (VPD, kPa), respectively. Fraction f_{min} is the minimum daylight g_{sto} under field conditions expressed as a fraction of g_{max}. Variation in stomatal conductance with leaf age is described by f_{phen}, which modified g_{max} as a function of time within leaf duration. Further details on f_{phen}, f_{light}, f_{temp} and f_{VPD} calculations are provided in LRTAP (2017).

Finally, the POD$_Y$ (mmol m^{-2} PLA), expressed as the stomatal flux of O_3 accumulated over threshold Y (nmol O_3 m^{-2} s^{-1}) during the accumulation period of the experiment (from 26 June to 30 September 2016) was calculated from hourly data as:

$$PODY = \sum_{i=1}^{n} \max[Fst - Y, 0] \cdot \Delta t \tag{3}$$

where F_{st} is the stomatal O_3 flux (in nmol m^{-2} PLA s^{-1}), Y is the threshold, and $\Delta t = 1$ h (LRTAP, 2017).

2.5. Parameterization of functions for the three species

The three species were parameterized for the functions f_{phen}, f_{light}, f_{temp}, and f_{VPD}. Boundary lines of the relative g_s values (g_s/g_{max} for water) were calculated by an iterative process minimizing the normalized root-mean-square error (NRMSE). Each parameter was allowed to vary within plausible ranges taken from the literature for trees (e.g., LRTAP, 2017). A fine-tuning was finally applied in order to improve the fitting of the modeled g_s (using all the calculated parameters together) against measured g_s values. A function accounting for the soil water content effect on g_s was not considered necessary because all the plants were well irrigated, given that irrigation is a common practice in urban plants.

2.6. Relative responses calculation and statistical analysis

Relative responses for A_{sat} (R-A_{sat}) for different AOTX and POD$_Y$ thresholds were calculated. For each plant species and the two measuring times, first order regressions ($y = ax + b$) of A_{sat} with AOTX and POD$_Y$ values were performed in order to obtain the y-intercept (i.e., the hypothetically maximum value of the variable at zero O_3 exposure or uptake). Relative values for A_{sat} were therefore calculated as their actual values divided by their corresponding y-intercept. In this way, relative values become comparable on a common relative scale (Feng et al., 2012). Finally, the relationships between the calculated R-A_{sat} values and the AOTX and POD$_Y$ were determined using first order linear regressions. R^2 value of the relationships was considered as the main indicator of the performance of the different thresholds.

All the calculations and statistical tests were carried out with R (R Core Team, 2015). Regressions were considered significant at a P-value ≤ 0.05.

3. Results

3.1. Parameterization of the three species

The three species were parameterized (Table 1). A parameterization for the whole growing season of the plants was provided although it has to be noted that for POD$_Y$ calculation the accumulation period was from 26 June to 30 September 2016; the start and end of the growing season (SGS and EGS) were estimated based on local observations. PO was the species showing higher maximum stomatal conductance for O_3 (g_{max}), followed by FC, while g_{max} values for RP were about 30% lower than those of PO. Comparison of measured and modeled g_{sto} values allowed testing the performance of these parameterizations for estimating g_{sto} by applying f_{temp}, f_{VPD} and f_{phen} functions, both in terms of R^2 and NRMSE (Fig. 1). The higher the g_{max}, the higher the performance of the model estimations (R^2 from 0.51 in RP to 0.60 in PO, and NRMSE from 88.8 to 64.8 for the same species), which uncovers a higher difficulty for a good parameterization of the species when g_{sto} varied within a narrower range.

3.2. Exposure- and flux-response relationships for different thresholds

The performance of the fitting of the regressions between A_{sat} and AOTX index in terms of R^2 and intercept (i.e., the better when R^2 the closer to 1 and the intercept the closer to 100) was tested for different AOTX thresholds, from 0 to 60 ppb (Fig. 2). Responses were different for the three species. FC showed the highest R^2 values (0.904) at AOT60, while the highest R^2 for PO and RP were 0.868 and 0.876 and occurred at higher thresholds, 55 ppb and 30 ppb, respectively (Table 2). The corresponding intercepts for FC, PO and RP were 100.6%, 99.2% and 96.6%, respectively. AOT40 should be the best common metric for the three species, given that the three species showed similar R^2 values (between 0.838 and 0.868) at threshold 40 ppb, as shown by the crossing of the three lines of Fig. 2. For AOT40 metric, the intercepts of the

Table 1
Parameterization for the stomatal conductance model for the three species. The terminology is based on LRTAP (2017). The values in brackets are "dummy" values required for modeling purposes in plants without a mid-season dip in f_{phen} (see LRTAP, 2017 for further details).

Parameter	Units	FC	PO	RP
g_{max}	mmol O_3 m^{-2} PLA s^{-1}	203	225	152
T_{min}	°C	8	8	10
T_{opt}	°C	22	22	22
T_{max}	°C	42	41	40
Light$_a$	–	0.003	0.004	0.005
VPD_{max}	kPa	1.5	1.5	3
VPD_{min}	kPa	4	5	5.5
f_{min}	(Fraction of g_{max})	0.01	0.01	0.01
A_{start_FD} (SGS)	(DOY)	105	105	105
A_{end_FD} (EGS)	(DOY)	270	270	270
f_{phen_a}	(Fraction of g_{max})	0	0	0
f_{phen_b}	(Fraction of g_{max})	(1)	(1)	(1)
f_{phen_c}	(Fraction of g_{max})	1	1	1
f_{phen_d}	(Fraction of g_{max})	(1)	(1)	(1)
f_{phen_e}	(Fraction of g_{max})	0.01	0.2	0.02
$f_{phen\_1\_FD}$	(No. of days)	39	30	30
$f_{phen\_2\_FD}$	(No. of days)	(180)	(180)	(180)
$f_{phen\_3\_FD}$	(No. of days)	(180)	(180)	(180)
$f_{phen\_4\_FD}$	(No. of days)	50	40	80
LIM_{start_FD}	(No. of days)	(0.0)	(0.0)	(0.0)
LIM_{end_FD}	(No. of days)	(0.0)	(0.0)	(0.0)

regression lines were 100.0%, 98.5% and 97.7% for FC, PO and RP, respectively.

For R-A_{sat} responses against flux metrics, the highest R^2 were observed for FC at POD$_7$ ($R^2 = 0.863$), for PO at POD$_5$ ($R^2 = 0.728$), and for RP at POD$_1$ ($R^2 = 0.911$) (Fig. 2, Table 2). The corresponding intercepts for the regression lines were 100.2%, 99.6% and 98.5%, for FC, PO and RP, respectively. Using POD$_1$ metric, the reference metric for establishing the O_3 CL for trees (LRTAP, 2017), the resulting R^2 values would be 0.781, 0.728 and 0.911 for FC, PO and RP, respectively, and their corresponding intercepts would be 102.4%, 96.5% and 98.5%, respectively.

Selecting the thresholds with the best fittings with R-A_{sat} for both exposure- and flux-based metrics, it was observed that AOTX metric performed better than POD$_Y$ metric for FC in terms of R^2 but the contrary held true for PO and RP: for FC, R^2 value of AOT60 > R^2 value of POD7, but R^2 of POD$_5$ > R^2 of AOT55 for PO, and R^2 of POD$_1$ > R^2 of AOT30 for RP (Table 2). On the other hand, using the same metrics, AOT40 and POD$_1$, it was possible to compare the slopes of their regressions with R-A_{sat}, and use these slope values as indicative of the O_3 sensitivity of the species. Our results suggest that the ranking from higher to lower O_3 sensitivity was RP > FC > PO (Table 2).

3.3. Contributions of the different O_3 concentrations to the POD$_Y$ values

The minimum O_3 concentrations that contributed to these O_3 fluxes were 39 ppb, 25 ppb and 8 ppb for FC, PO and RP, respectively (Fig. 3). Consistently, the lower the Y threshold selected for the species (7, 5 and 1 nmol O_3 m^{-2} s^{-1} for FC, PO and RP, respectively), the lower the O_3 concentration values that can contribute to the accumulated O_3 fluxes.

4. Discussion

In the last decade, O_3 risk assessment has shifted from exposure to flux-based metric, i.e., what is relevant for the plant in terms of O_3 effects is the O_3 uptake by the plants through the stomata, rather than the O_3 concentrations present in the atmosphere (Matyssek et al., 2007; Mills et al., 2011; Büker et al., 2015). As this approach takes into account influences of meteorological, soil moisture and phenological factors on the O_3 uptake by the plants, the performance of the flux-based index POD$_Y$ has been reported to be frequently superior to AOTX (e.g., Karlsson et al., 2007; Hu et al., 2015). This is particularly
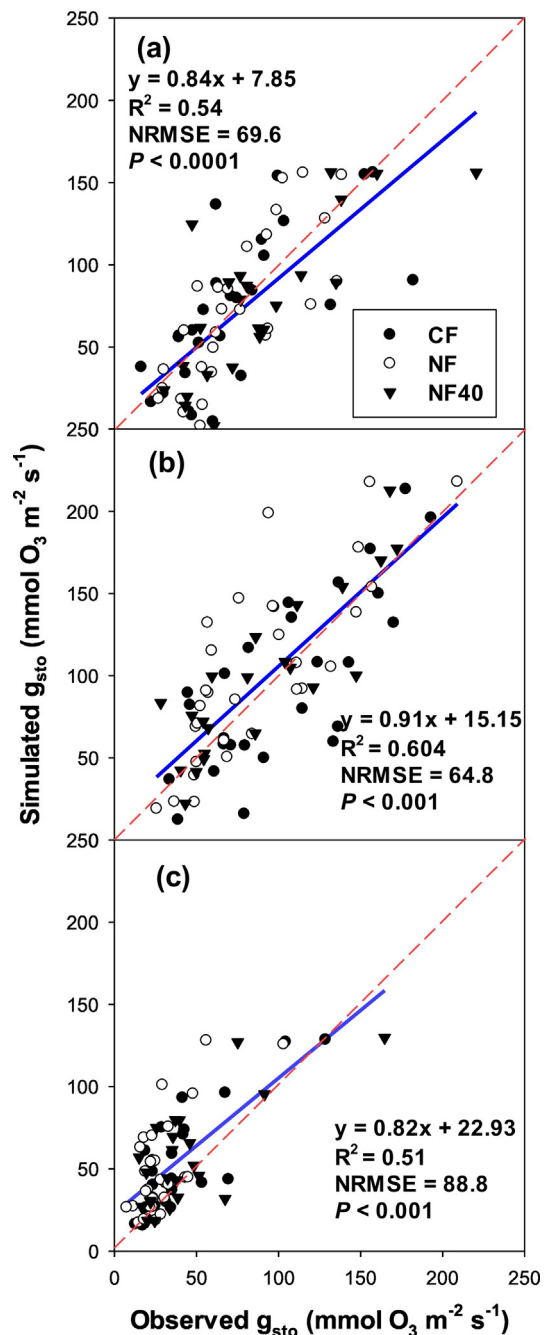

Fig. 1. Performance of the fitting of modeled stomatal conductance with measured values for the three species. (a), *Fraxinus chinensis* (FC); (b), *Platanus orientalis* (PO); (c), *Robinia pseudoacacia*. NRMSE, Normalized Root-Mean-Square Error.

true when water stress limits O_3 uptake by the plants as reported by Gao et al. (2017) for poplar or by Hoshika et al. (2017) for oak species. In our experiment, plants were well irrigated in order to avoid water stress; therefore a soil moisture function accounting for the stomatal conductance reduction due to limited water availability was not included in the current stomatal conductance model. Under such conditions, both the best AOTX and POD$_Y$ relationships for each species performed very well for predicting decreases in R-A_{sat}: R^2 values were always above 0.868 for AOTX metric and results were very similar for POD$_Y$ metric (R^2 above 0.863) (Table 2). For FC, AOT60 was the metric showing better fitting with R-A_{sat} in terms of R^2 while POD$_5$ and POD$_1$ were the best metrics for PO and RP, respectively. As it is desirable that the intercepts of the regression equations are as close as possible to 100%, in this sense the POD$_Y$ was slightly superior to AOTX, as for the three
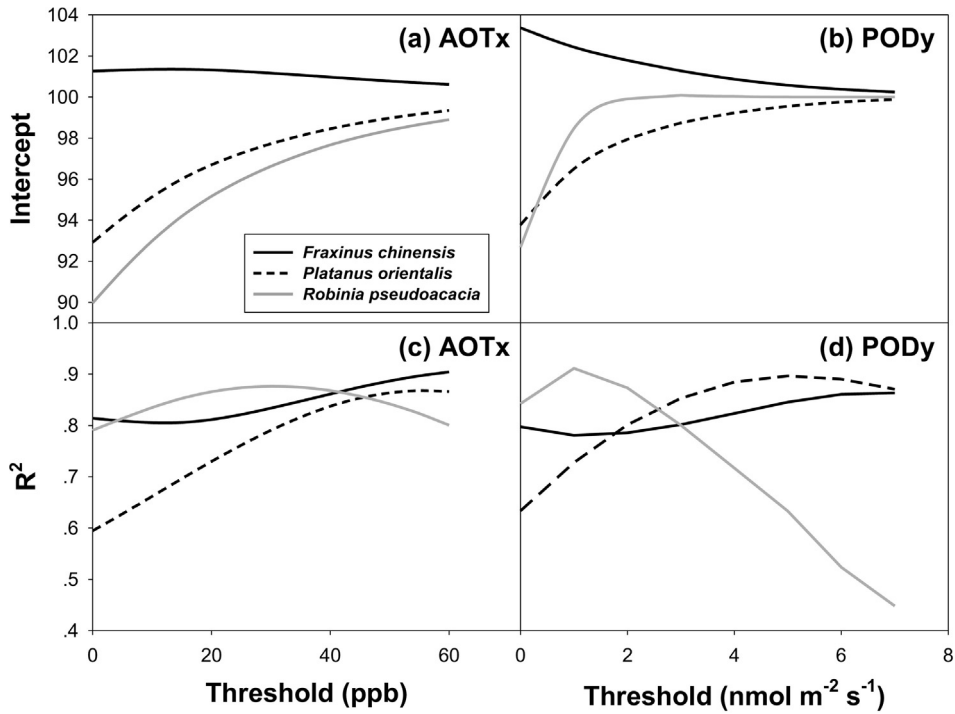
Fig. 2. R^2 and intercepts of the regressions between exposure and O_3 flux metrics with A_{sat} at different thresholds for the three species.

species the POD_Y intercepts ranged between 98.5%–100.2% against 96.6%–100.6% for AOTX. Therefore, it can be concluded that considering all the species together, flux-based metrics were in general slightly better at predicting R-A_{sat} changes due to O_3 and should be preferred over AOTX metric. Similarly, Bagard et al. (2015) studied the relationships of CO_2 assimilation against AOTX and POD_Y in two crops and a poplar clone, and also found a modest improvement using the flux approach. In any case, given that AOTX metrics also performed well, it would be also reasonable to use AOTX metrics for estimating O_3 impacts on A_{sat} in these three species when insufficient data are available for stomatal O_3 flux modeling.

When establishing relationships with R-A_{sat}, the use of a common threshold for AOTX and also for POD_Y in the three species allows a comparison of their sensitivity to O_3. For this comparison AOT40 and POD_1 were selected as both tresholds have been commonly used for trees (LRTAP, 2017). Using the slope of the regression as indicator of the sensitivity of the species, for both AOT40 and POD_1 metrics, similar

Table 2
Exposure and O_3 flux metrics, their equations and R^2 values, for the thresholds with the best fittings of the regressions with R-A_{sat}. The same information is also provided for AOT40 and POD_1, for comparative purposes among species. For the equations, AOTX unit is ppb h and POD_Y unit is mmol m^{-2}.

Species	Metric	Equation	R2	P value
Best AOTX and POD_Y metrics				
FC	AOT60	$y = -0.0016x + 100.6$	0.904	<0.001
PO	AOT55	$y = -0.0013x + 99.2$	0.868	<0.001
RP	AOT30	$y = -0.0015x + 96.6$	0.876	<0.001
FC	POD_7	$y = -16.8x + 100.2$	0.863	<0.001
PO	POD_5	$y = -5.67x + 99.6$	0.897	<0.001
RP	POD_1	$y = -13.46x + 98.5$	0.911	<0.001
Metrics for comparison (AOT40 and POD_1)				
FC	AOT40	$y = -0.0011x + 101$	0.861	<0.001
PO	AOT40	$y = -0.001x + 98.5$	0.838	<0.001
RP	AOT40	$y = -0.0017x + 97.7$	0.868	<0.001
FC	POD_1	$y = -4.57x + 102.4$	0.781	<0.001
PO	POD_1	$y = -2.82x + 96.5$	0.728	<0.01
RP	POD_1	$y = -13.46x + 98.5$	0.911	<0.001

conclusions can be drawn: PO was more tolerant than FC and the most sensitive species was RP. However, it is interesting to note that when AOT40 was used, the differences in the slopes of RP with the other two species was lower (-0.0017 for RC against -0.0011 and -0.0010 for FC and PO, respectively) than when POD_1 was the reference metric (-13.46 for RP against -4.57 and -2.82 for FC and PO, respectively). In other words, for the same accumulated O_3 fluxes, the decline of the relative A_{sat} was much higher in RP than in FC and PO. In this regard, as shown here, it has to be underlined that species sensitivity was not related to the species-specific g_{max}. This mismatching between g_{max} and sensitivity has been often observed in different experiments (e.g., Feng et al., 2016) as the sensitivity to O_3 is also dependent on the antioxidant capacity of the species (Li et al., 2016), as well as leaf traits such as the Leaf Mass per Area or anatomical features affecting the pollutant diffusivity throughout the leaf mesophyll (e.g. Gerosa et al., 2009; Li et al., 2016). It has to be noted that the magnitude of the reductions in A_{sat} against both metrics is much higher than the reductions observed for biomass in other tree species (e.g., Mills et al., 2011; Hu et al., 2015). This is consistent with Shang et al. (2017), who observed that photosynthetic parameters showed changes both at lower accumulated O_3 fluxes and more severe than other variables such as leaf morphological treats and biomass. On the other hand, the sensitivity of RP to O_3 has been previously highlighted as an O_3 bioindicator in the USA (Innes et al., 2001) and RP showed visible symptoms under ambient O_3 levels in China (Feng et al., 2014). Field symptoms, however, have also been found in FC in Beijing area (Feng et al., 2014).

For flux-based metrics, thresholds have been introduced in order to account for the instantaneous O_3 flux detoxification capacity of the plants (Mills et al., 2011). The fact that the most sensitive species showed the best threshold for the fitting between R-A_{sat} and POD_Y at a $Y = 1$ nmol·m^{-2}·s^{-1}, while the most tolerant showed the best fittings at a Y of 5 or 7 nmol·m^{-2}·s^{-1}, might suggest that the Y threshold for the best fitting would be indicative of plant sensitivity, and that species with higher thresholds would have a higher antioxidant capacity. However, such a conclusion may be inaccurate, as indicated by the fact that the species with higher g_{max} values perform better at higher O_3
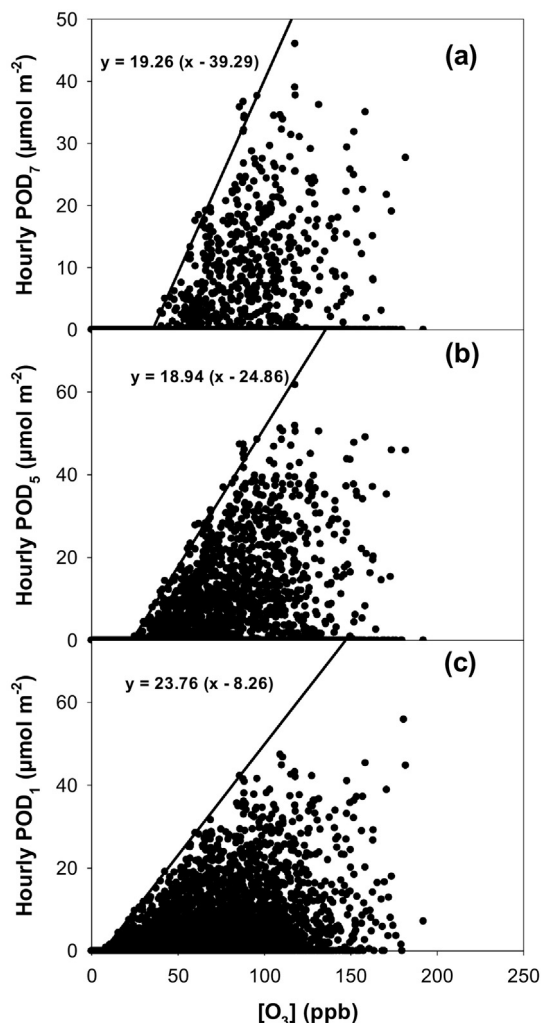
Fig. 3. Hourly POD_Y values over the selected thresholds for the three species in relation to the hourly O_3 concentrations (ppb) that contributed to these hourly POD_Y. (a), *Fraxinus chinensis* (FC); (b), *Platanus orientalis* (PO); (c), *Robinia pseudoacacia*.

thresholds. Thresholds in the range of 6–7 nmol O_3 m^{-2} s^{-1} have been proposed for the CLs of crops or fast growing trees e.g. poplar (Mills et al., 2011; Hu et al., 2015). And fast-growing species such as poplar are known to be more responsive to O_3 than slower-growing species such as beech (Bortier et al., 2000), for which a CL based on POD_1 has been proposed (LRTAP, 2017). Therefore, the best threshold in terms of R^2 of the relationship between R-A_{sat} and POD_Y cannot be used for comparing species sensitivity or antioxidant capacity, at least among species with different g_{max} values.

Interestingly, higher thresholds for POD_Y imply that only higher O_3 concentration contributes to the POD_Y. In the present study, O_3 concentrations higher than 39 ppb, 25 ppb and 8 ppb started to accumulate to the POD_7, $POD5$ and POD_1 for FC, PO and RP, respectively; therefore they are likely to affect A_{sat}. For each species, the concentrations slightly above these O_3 concentration thresholds will have a small contribution to the POD_Y even if g_{sto} is close to g_{max}. However, at higher O_3 concentrations the contribution to POD_Y could be much higher, being limited by g_{sto} to the extent of g_{max} (Zhang et al., 2017). Given that even the highest of these three O_3 concentrations thresholds is commonly exceeded in China, even in garden areas inside large cities such as Beijing (Chen et al., 2015b), current ambient O_3 levels are expected to have a negative impact on the photosynthesis of these three species, and in particular on that of RP, and finally on biomass. As information on O_3 effects caused by accumulated stomatal O_3 fluxes may be a concept somewhat

difficult to transfer to policy-makers and practitioners, we think that linking stomatal O_3 fluxes with the O_3 concentrations contributing to them may be helpful as a support for communicating this kind of results.

Species with relatively high g_{max} values such as FC and PO may have a potentially higher removal capacity of O_3 and other gaseous pollutants through stomatal uptake. Furthermore, if they are low BVOC emitters as it is the case of FC (Aydin et al., 2014, Yuan et al., unpublished), these plants can be particularly suitable for providing beneficial effects on urban air quality (Calfapietra et al., 2013; Ghirardo et al., 2016). Parameters of stomatal deposition models, together with other parameters such as the Leaf Area Index (LAI) and measures of the distribution and density of the urban species, are necessary for accurately modeling the removal capacity of gaseous pollutants by urban vegetation (Bottalico et al., 2017). Ideally, however, for the parameterization to be robust and valid for different areas, they should be based on data from different experiments conducted under different climatic conditions.

5. Conclusion

In terms of both potential air pollution removal capacity and O_3 sensitivity, FC and PO are more suitable than RP for planting in gardens or periurban areas where O_3 levels can be relatively high. Efforts for parameterizing the stomatal conductance of the main urban tree species and characterizing their relative sensitivity to O_3 as shown in the present study should be made in order to support the modeling of pollutant uptake by urban vegetation and ultimately the decision-making by practitioners for green urban planning. In any case, these green solutions for air pollution abatement should be regarded as complementary and not as a surrogate of actions addressed to effectively reduce pollutant emissions, given that the contribution of plants to improve air quality, although environmentally and economically relevant, remains modest (typically in the range of 1% to 5%, cf. Nowak, 2006; Escobedo and Nowak, 2009).

References

Aydin, Y.M., Yaman, B., Koca, H., Dasdemir, O., Kara, M., Altiok, H., Dumanoglu, Y., Bayram, A., Tolunay, D., Odabasi, M., Elbir, T., 2014. Biogenic volatile organic compound (BVOC) emissions from forested areas in Turkey: determination of specific emission rates for thirty-one tree species. Sci. Total Environ. 490, 239–253.

Bagard, M., Jolivet, Y., Hasenfratz-Sauder, M.P., Gerard, J., Dizengremel, P., Le Thiec, D., 2015. Ozone exposure and flux-based response functions for photosynthetic traits in wheat, maize and poplar. Environ. Pollut. 206, 411–420.

Bortier, K., Ceulemans, R., De Temmerman, L., 2000. Effects of ozone exposure on growth and photosynthesis of beech seedlings (*Fagus sylvatica*). New Phytol. 146, 271–280.

Bottalico, F., Travaglini, D., Chirici, G., Garfi, V., Giannetti, F., De Marco, A., Fares, S., Marchetti, M., Nocentini, S., Paoletti, E., Salbitano, F., Sanesi, G., 2017. A spatially-explicit method to assess the dry deposition of air pollution by urban forests in the city of Florence, Italy. Urban For. Urban Green. 27, 221–234.

Büker, P., Feng, Z., Uddling, J., Briolat, A., Alonso, R., Braun, S., Elvira, S., Gerosa, G., Karlsson, P.E., Le Thiec, D., 2015. New flux based dose–response relationships for ozone for European forest tree species. Environ. Pollut. 206, 163–174.

Calfapietra, C., Fares, S., Manes, F., Morani, A., Sgrigna, G., Loreto, F., 2013. Role of biogenic volatile organic compounds (BVOC) emitted by urban trees on ozone concentration in cities: a review. Environ. Pollut. 183, 71–80.

Chen, W., Tang, H., Zhao, H., 2015a. Diurnal, weekly and monthly spatial variations of air pollutants and air quality of Beijing. Atmos. Environ. 119, 21–34.

Chen, W., Yan, L., Zhao, H., 2015b. Seasonal variations of atmospheric pollution and air quality in Beijing. Atmosphere 6 (12), 1753–1770.

Cieslik, S., Tuovinen, J.-P., Baumgarten, M., Matyssek, R., Brito, P., Wieser, G., 2013. Gaseous exchange between forests and the atmosphere. Climate Change, Air Pollution and Global Challenges. Developments in Environmental Science 13. Elsevier, pp. 19–36.

Cooper, O.R., Parrish, D.D., Ziemke, J., Balashov, N.V., Cupeiro, M., Galbally, I.E., Gilge, S., Horowitz, L., Jensen, N.R., Lamarque, J.-F., Naik, V., Oltmans, S.J., Schwab, J., Shindell, D.T., Thompson, A.M., Thouret, V., Wang, Y., Zbinden, R.M., 2014. Global distribution and trends of tropospheric ozone: an observation-based review. Elem. Sci. Anth. 2, 000029.

Core Team, R., 2015. R: A language and environment for statistical computing. R Foundation for Statistical Computing, Vienna, Austria. URL:. http://www.R-project.org/.

Emberson, L., Wieser, G., Ashmore, M., 2000. Modelling of stomatal conductance and ozone flux of Norway spruce: comparison with field data. Environ. Pollut. 109, 393–402.

Escobedo, F.J., Nowak, D.J., 2009. Spatial heterogeneity and air pollution removal by an urban forest. Landsc. Urban Plan. 90, 102–110.

Feng, Z., Tang, H., Uddling, J., Pleijel, H., Kobayashi, K., Zhu, J., Oue, H., Guo, W., 2012. A stomatal ozone flux-response relationship to assess ozone-induced yield loss of winter wheat in subtropical China. Environ. Pollut. 164, 16–23.

Feng, Z., Sun, J., Wan, W., Hu, E., Calatayud, V., 2014. Evidence of widespread ozone-induced visible injury on plants in Beijing, China. Environ. Pollut. 193, 296–301.

Feng, Z., Hu, E., Wang, X., Jiang, L., Liu, X., 2015. Ground-level O_3 pollution and its impacts on food crops in China: a review. Environ. Pollut. 199, 42–48.

Feng, Z., Wang, L., Pleijel, H., Zhu, J., Kobayashi, K., 2016. Differential effects of ozone on photosynthesis of winter wheat among cultivars depend on antioxidative enzymes rather than stomatal conductance. Sci. Total Environ. 572, 404–411.

Gao, F., Calatayud, V., García-Breijo, F., Reig-Armiñana, J., Feng, Z., 2016. Effects of elevated ozone on physiological, anatomical and ultrastructural characteristics of four common urban tree species in China. Ecol. Indic. 67, 367–379.

Gao, F., Catalayud, V., Paoletti, E., Hoshika, Y., Feng, Z., 2017. Water stress mitigates the negative effects of ozone on photosynthesis and biomass in poplar plants. Environ. Pollut. 230, 268–279.

Gerosa, G., Finco, A., Mereu, S., Vitale, M., Manes, F., Denti, A.B., 2009. Comparison of seasonal variations of ozone exposure and fluxes in a Mediterranean Holm oak forest between the exceptionally dry 2003 and the following year. Environ. Pollut. 157, 1737–1744.

Ghirardo, A., Xie, J., Zheng, X., Wang, Y., Grote, R., Block, K., Wildt, J., Mentel, T., Kiendler-Scharr, A., Hallquist, M., Butterbach-Bahl, K., Schnitzler, J.P., 2016. Urban stress-induced biogenic VOC emissions and SOA-forming potentials in Beijing. Atmos. Chem. Phys. 16, 2901–2920.

Hoshika, Y., Moura, B., Paoletti, E., 2017. Ozone risk assessment in three oak species as affected by soil water availability. Environ. Sci. Pollut. Res. Int. http://dx.doi.org/10.1007/s11356-017-9786-7.

Hu, E., Gao, F., Xin, Y., Jia, H., Li, K., Hu, J., Feng, Z., 2015. Concentration- and flux-based ozone dose-response relationships for five poplar clones grown in North China. Environ. Pollut. 207, 21–30.

Innes, J.L., Skelly, J.M., Schaub, M., 2001. Ozone and Broadleaved Species. A Guide to the Identification of Ozone-induced Foliar Injury. Birmensdorf, Eidgenossische Forschungsanstalt WSL, Bern, Stuttgart, Wien. Haupt (136 pp.).

Jarvis, P., 1976. The interpretation of the variations in leaf water potential and stomatal conductance found in canopies in the field. Philos. Trans. R. Soc. Lond. Ser. B Biol. Sci. 273 (927), 593–610.

Karlsson, P.E., Braun, S., Broadmeadow, M., Elvira, S., Emberson, L., Gimeno, B.S., Le Thiec, D., Novak, K., Oksanen, E., Schaub, M., Uddling, J., Wilkinson, M., 2007. Risk assessments for forest trees: the performance of the ozone flux versus the AOT concepts. Environ. Pollut. 146, 608–616.

Li, P., Calatayud, V., Gao, F., Uddling, J., Feng, Z., 2016. Differences in ozone sensitivity among woody species are related to leaf morphology and antioxidant levels. Tree Physiol. 36, 1105–1116.

Loreto, F., Fares, S., 2013. Biogenic volatile organic compounds and their impacts on biosphere–atmosphere interactions. Climate Change, Air Pollution and Global Challenges. Developments in Environmental Science 13. Elsevier, pp. 57–75.

LRTAP, 2017. Mapping critical levels for vegetation, chapter III of manual on methodologies and criteria for modelling and mapping critical loads and levels and air pollution effects, risks and trends. UNECE convention on long-range transboundary air pollution. On web at. www.icpmapping.org, Accessed date: 5 September 2017.

Matyssek, R., Bytnerowicz, A., Karlsson, P.E., Paoletti, E., Sanz, M., Schaub, M., Wieser, G., 2007. Promoting the O_3 flux concept for European forest trees. Environ. Pollut. 146, 587–607.

Mills, G., Pleijel, H., Braun, S., Büker, P., Bermejo, V., Calvo, E., Danielsson, H., Emberson, L., Fernández, I.G., Grünhage, L., Harmens, H., Hayes, F., Karlsson, P.-E., Simpson, D., 2011. New stomatal flux-based critical levels for ozone effects on vegetation. Atmos. Environ. 45, 5064–5068.

Nowak, D.J., 2006. Institutionalizing urban forestry as a "biotechnology" to improve environmental quality. Urban For. Urban Green. 5 (2), 93–100.

Nowak, D.J., Hirabayashi, S., Bodine, A., Greenfield, E., 2014. Tree and forest effects on air quality and human health in the United States. Environ. Pollut. 193, 119–129.

Paoletti, E., De Marco, A., Beddows, D.C., Harrison, R.M., Manning, W.J., 2014. Ozone levels in European and USA cities are increasing more than at rural sites, while peak values are decreasing. Environ. Pollut. 192, 295–299.

Shang, B., Feng, Z., Li, P., Yuan, X., Xu, Y., Calatayud, V., 2017. Ozone exposure- and flux-based response relationships with photosynthesis, leaf morphology and biomass in two poplar clones. Sci. Total Environ. 603–604, 185–195.

Sicard, P., De Marco, A., Troussier, F., Renou, C., Vas, N., Paoletti, E., 2013. Decrease in surface ozone concentrations at Mediterranean remote sites and increase in the cities. Atmos. Environ. 79, 705–715.

Sun, J., Feng, Z., Ort, D.R., 2014. Impacts of rising tropospheric ozone on photosynthesis and metabolite levels on field grown soybean. Plant Sci. 226, 147–161.

The Royal Society, 2008. Ground-level ozone in the 21st century: future trends, impacts and policy implications. Science Policy REPORT 15/08. The Royal Society, p. 148.

Wang, Z., Li, Y., Chen, T., Zhang, D., Sun, F., Wei, Q., Dong, X., Sun, R., Huan, N., Pan, L., 2015. Ground-level ozone in urban Beijing over a 1-year period: temporal variations and relationship to atmospheric oxidation. Atmos. Res. 164–165, 110–117.

Wang, W.N., Cheng, T.H., Gu, X.F., Chen, H., Guo, H., Wang, Y., Bao, F.W., Shi, S.Y., Xu, B.R., Zuo, X., Meng, C., Zhang, X.C., 2017. Assessing spatial and temporal patterns of observed ground-level ozone in China. Sci Rep http://dx.doi.org/10.1038/s41598-017-03929-w.

Wittig, V.E., Ainsworth, E.A., Long, S.P., 2007. To what extent do current and projected increases in surface ozone affect photosynthesis and stomatal conductance of trees? A meta-analytic review of the last 3 decades of experiments. Plant Cell Environ. 30, 1150–1162.

Yang, J., McBride, J., Zhou, J., Sun, Z., 2005. The urban forest in Beijing and its role in air pollution reduction. Urban For. Urban Green. 3, 65–78.

Zhang, W., Feng, Z., Wang, X., Liu, X., Hu, E., 2017. Quantification of ozone exposure- and stomatal uptake-yield response relationships for soybean in Northeast China. Sci. Total Environ. 599–600, 710–720.